Patterns in seismic anisotropy driven by rollback subduction beneath the High Lava Plains

K. A. Druken,[1] M. D. Long,[2] and C. Kincaid[1]

Received 24 March 2011; revised 25 May 2011; accepted 31 May 2011; published 8 July 2011.

[1] We present three-dimensional laboratory modeling of the evolution of finite strain and compare these to shear wave splitting observations in the Northwest U.S. under the High Lava Plains (HLP). We show that relationships between mantle flow and anisotropy are complicated in subduction zones and factors such as initial orientation of the olivine fast-axis, style of subduction, and time evolving flow are important. Due to increased horizontal shear, systems with a component of rollback subduction have simple trench-normal strain alignment within the central region of the backarc mantle wedge while those with more simple longitudinal sinking are often variable and complex. In the HLP, splitting observations are consistent with rollback-driven laboratory results. **Citation:** Druken, K. A., M. D. Long, and C. Kincaid (2011), Patterns in seismic anisotropy driven by rollback subduction beneath the High Lava Plains, *Geophys. Res. Lett.*, *38*, L13310, doi:10.1029/2011GL047541.

1. Introduction

[2] The High Lava Plains (HLP) region of eastern and central Oregon has been the site of voluminous intraplate volcanism over the past ~17 Ma (Figure 1a), but the causes of this volcanic activity remain poorly understood. Various explanations for the vigorous tectonomagmatism of the HLP have been proposed, which generally invoke the rollback and steepening of the Cascadia slab, the effect of the putative Yellowstone plume, or lithospheric structure or processes [e.g., *Cross and Pilger*, 1978; *Carlson and Hart*, 1987; *Camp and Ross*, 2004; *Jordan et al.*, 2004]. Models and observations of the pattern of upper mantle flow can help test the plausibility of explanations for the origin and evolution of the HLP.

[3] In this study we combine geodynamic models of subduction-related mantle flow with observations of seismic anisotropy [e.g., *Fischer et al.*, 2000; *Conder and Wiens*, 2007] to show that flow beneath the HLP is plate-driven and controlled by the rollback, steepening, and downdip motion of the Cascadia slab. Seismic anisotropy in the upper mantle is a consequence of lattice-preferred orientation (LPO) of olivine and observations of anisotropy can yield relatively direct constraints on mantle flow patterns if the relationship between strain and anisotropy is well known [e.g., *Karato et al.*, 2008; *Long and Becker*, 2010]. In subduction zones, observations from shear wave splitting studies are often complex and variable, with many regions dominated by trench-parallel fast directions; in contrast, the Cascadia subduction zone is mostly dominated by trench-normal splitting [e.g., *Long and Silver*, 2008].

[4] We compare makers of finite strain within laboratory subduction experiments to measurements of fast SKS splitting directions, which indicate the local orientation of upper mantle anisotropy beneath the HLP. We use single-station average SKS fast directions for stations of the HLP broadband seismic experiment [*Carlson et al.*, 2005] and USArray Transportable Array stations. The splitting measurements come from the data set of *Long et al.* [2009], augmented with new measurements from an additional 15 HLP stations. *Long et al.* [2009] identified strong splitting with large delay times (1.5–2.5 sec) and roughly E-W fast directions. Given the thin lithosphere beneath the region [*Warren et al.*, 2008; *Wagner et al.*, 2010], these simple splitting patterns are almost certainly associated with contemporary mantle flow in the asthenosphere beneath the HLP, and a direct comparison of whisker orientations from the flow models and SKS fast splitting directions is appropriate (refer to *Long et al.* [2009] for full discussion on interpretation of splitting results).

2. Laboratory Model

[5] We examine the evolution of finite strain within 3-D subduction-driven flow using a kinematic laboratory model [*Kincaid and Griffiths*, 2003, 2004] (Figure 1b). The upper 2400 km of the mantle is modeled using glucose syrup held within a transparent Perspex acrylic tank (100 cm × 60 cm × 40 cm) and a rigid Phenolic sheet (20 cm wide × 2.5 cm thick) is used to model the slab. Two hydraulic pistons attached to the slab control downdip (U_D) and translational (U_T) motions while a third controls the slab dip angle with time (θ_t). Although plate motions are kinematic, they are designed to mimic the range of sinking styles observed dynamically [e.g., *Kincaid and Olson*, 1987; *Griffiths et al.*, 1995; *Funiciello et al.*, 2003; *Schellart*, 2004]. With the exception of the slab steepening cases, an average slab dip for the Cascadia system of ~60° [e.g., *Xue and Allen*, 2010] was chosen and remained constant across all experiments. Plate rates are scaled similarly to *Kincaid and Griffiths* [2003, 2004] using the Péclet number, $\mathrm{Pe} = U_D D \kappa^{-1}$, where D and κ represent the relevant length scale and thermal diffusivity of the slab ($\kappa_{lab} \sim 10^{-3}$ cm^2 s^{-1} and $\kappa_{mantle} \sim 10^{-2}$ cm^2 s^{-1}), respectively. In this study, the characteristic length scale (D) is chosen to represent a 1200 km wide trench, so that 1 cm in the experiment is equivalent to 60 km in the mantle. Plate rates of 3–5 cm/min in the laboratory correspond to rates of 2.6–4.4 cm/yr in the

[1]Graduate School of Oceanography, University of Rhode Island, Narragansett, Rhode Island, USA.
[2]Department of Geology and Geophysics, Yale University, New Haven, Connecticut, USA.

0094-8276/11/2011GL047541

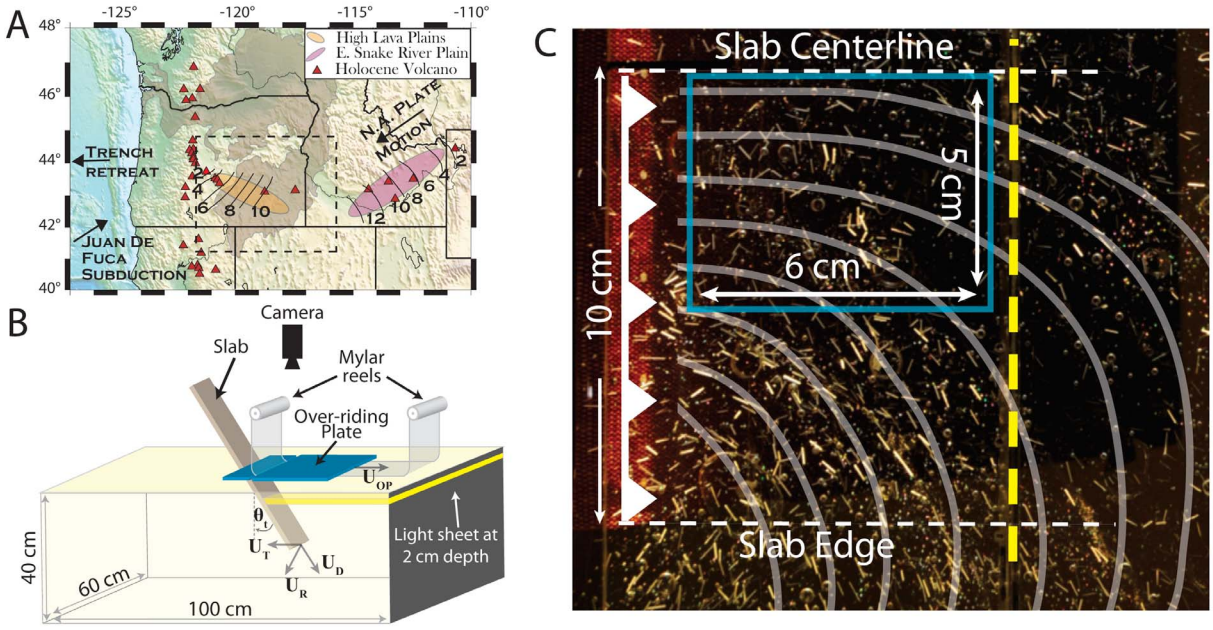

Figure 1. (a) Tectonic setting of the Pacific Northwest. The brown shaded region indicates the extent of the Columbia River/Steens flood basalts. Locations of Holocene volcanic centers are shown with red triangles. The approximate extent of the High Lava Plains (HLP) and Eastern Snake River Plain volcanic trends are shown; thin black lines indicate the approximate age contours of rhyolitic volcanism in each region [after *Jordan et al.*, 2004; *Christiansen et al.*, 2002]. Black arrows indicate the absolute plate motion direction of the North American plate, the convergence direction of the Juan de Fuca plate relative to North America, and the absolute migration of the Juan de Fuca trench, respectively. The dashed box indicates the study area in this study. (b) Cartoon sketch of the modified kinematic subduction model. See *Kincaid and Griffiths* [2003, 2004] for more details. (c) Map-view image of illuminated slice of whiskers during a typical experiment. The yellow dashed line and blue box indicate the overriding plate extension center and area of interest for this study. Approximate instantaneous streamlines for flow field shown in grey.

mantle. In all cases, the plate subducted within 0.5 cm of the base of the tank and for those with a translational component of motion (U_T), the trench retreated 22 cm (~1300 km).

[6] To achieve the no-slip surface condition imposed by the overriding lithosphere, an additional thin transparent Perspex plate migrates along the fluid surface with trench motion (Figure 1b, blue plate). As the slab retreats, a motorized spool of Mylar sheeting is used to create relative extension at the surface approximately 8.3 cm (~500 km) from the trench. Fluid in contact with the overriding plate on the trench-ward side of the extension center couples with the rollback rate (U_T), while the surface on the back-arc side of the extension center is influenced by the release rate of the Mylar (U_{op}). Absolute plate motion across the domain is trench-ward, however, on the back-arc side the plate speed is less than the rollback rate ($U_{op} < U_T$), producing relative extension.

[7] As with *Buttles and Olson* [1998], we utilize ~5 (±1) mm long synthetic paint brush hairs, or "whiskers", as passive markers for the local orientation of maximum finite strain (Figure 1c). *Buttles and Olson* [1998] showed that for upper mantle simple shear deformation, whiskers are a suitable laboratory analog for the orientation of the olivine anisotropic fast a-axis. During each experiment, whiskers were illuminated using a 1 cm (60 km) thick horizontal light sheet centered 2 cm (100 km) below the base of the lithosphere. High resolution still cameras were used to image whisker alignment at 5 second (570,000 yr) intervals and then manually digitized to track individual whisker orientations in space and time. The high resolution imaging allowed for very precise whisker identification within the illuminated layer to accuracies of approximately ±1 degree. Whisker orientation angles (ϕ) were normalized between 0 and 1, where Φ^* values of 0–0.33 (±0°–30°), 0.34–0.66 (±31°–60°), and 0.67–1.0 (±61°–90°) represent trench-parallel, intermediate and trench-normal alignment, respectively.

3. Alignment Results

[8] We present strain alignment results from a series of 10 experiments (Table 1) with varied styles of subduction (e.g., longitudinal vs. rollback sinking, extension of the overriding plate). Whiskers were uniformly distributed horizontally (no vertical component) within the upper ~5 cm of the fluid, with >90% of the whiskers initially oriented either (1) perpendicular (normal) or (2) parallel to the trench. For this study we examined whisker orientations within the central backarc region, which is away from the slab edges where strong trench-parallel flow occurs in cases of slab rollback (Figure 1c, blue box). We ignore areas close to the extension center and wedge apex where flow has a strong vertical component. Although the subduction-induced flow can be complex, the horizontal flow trajectories observed within the area of interest remained approximately trench-normal (60°–90°) over the duration of each experiment

Table 1. Experimental Parameters for Plate Forcings and Whisker Alignment[a]

	Subduction Parameters				Whisker Alignment			
						Φ*		
Exp	Ud (cm/min)	Ut (cm/min)	Uop (cm/min)	Dip (°)	Φ_i^*	‖ (%)	Int. (%)	⊥ (%)
32	5	-	-	60	1	1	10	89
35	5	-	-	60	0	20	38	42
33	5	3	-	60	1	3	17	80
28	5	3	-	60	0	6	15	79
23	5	3	1.5	60	1	0	20	80
29	5	3	1.5	60	0	6	25	69
34	5	3	asym.	60	1	6	6	88
30	5	3	asym.	60	0	3	17	80
25	5	3	1.5	θ_t	1	0	9	91
31	5	3	1.5	θ_t	0	5	21	74

[a]Columns 2–5 list the plate forcing conditions for each experiment with U_D and U_T representing the downdip (or longitudinal) and translational plate speeds. U_{op} represents the Mylar rate on the backarc side of the extension center. In the lab, 1 cm/min is approximately equivalent to 0.8 cm/yr. Overriding plate rate (U_{op}) of 'asym' denotes asymmetric extension with rates ranging −1.5–1.5 cm/min along the extension axis. Dip angle is given in degrees from horizontal or as parameter θ_t, which indicates slab steepening with time from 49° to 74° at $\theta_t = 2°$ min^{-1}. Column 6 lists the normalized initial orientation of whiskers prior to plate motions, where '0' is equal to trench-parallel and '1' is trench-normal. Columns 7–9 list percent trench-parallel (‖, Φ* = 0–0.33), intermediate (Int., Φ* = 0.34–0.66), and trench-normal (⊥, Φ* = 0.67–1) whisker alignment after 10 min (~70 Ma) of subduction.

(Figure 1c, grey lines illustrate approximate instantaneous streamlines for a rollback case). Table 1 summarizes the subduction parameters as well as the degree of parallel (‖), intermediate (Int.), and normal (⊥) whisker alignment after 10 min. (~70 Ma) of subduction for each experiment.

3.1. Longitudinal Subduction

[9] Laboratory models characterize how different levels of subduction complexity influence alignment patterns of finite strain markers evolving in 3-D flow fields. We begin with the simplest mode of subduction, which produces a relatively complicated linkage between seismic observations and mantle flow. Figure 2a shows late-stage (70 Ma) histograms of normalized whisker orientation (Φ*) for the purely longitudinal cases. Bars in black (Exp. 32) and blue (Exp. 35) represent the cases where the initial whisker orientation is trench-normal ($\Phi_i^* = 1$) and trench-parallel ($\Phi_i^* = 0$), respectively. Trench-normal alignment is quite high (89%) for Exp. 32, which is not surprising given that the strain markers originated in this preferred state. More interestingly, Exp. 35 ($\Phi_i^* = 0$, blue histogram) shows that perpendicular alignment is weak (47%) even after 70 Ma of subduction. The majority of whiskers remain oriented in the initial trench-parallel position (15%) or are in the transitioning intermediate phase (38%) despite the trench-normal flow trajectories.

3.2. Rollback Subduction

[10] As with the $\Phi_i^* = 1$(trench ⊥) longitudinal case (Exp. 32), all $\Phi_i^* = 1$ experiments with a translational component of rollback (U_T) show strong trench-normal alignment, with late-stage values ranging from 69–91% (Table 1). However, unlike longitudinal subduction, all rollback cases show strong normal alignment even when initially aligned trench-parallel ($\Phi_i^* = 0$). Figures 2b and 2c illustrate the rollback-induced perpendicular alignment for two selected scenarios: (1) downdip and rollback motions, $U_D + U_T$ (Exps. 33 & 28) and (2) downdip, rollback and asymmetric extension of the overriding plate, $U_D + U_T + U_{opAsym}$ (Exps. 34 & 30). In both scenarios, the distribution of alignment is shown to depend little on the initial orientation of the whiskers (black

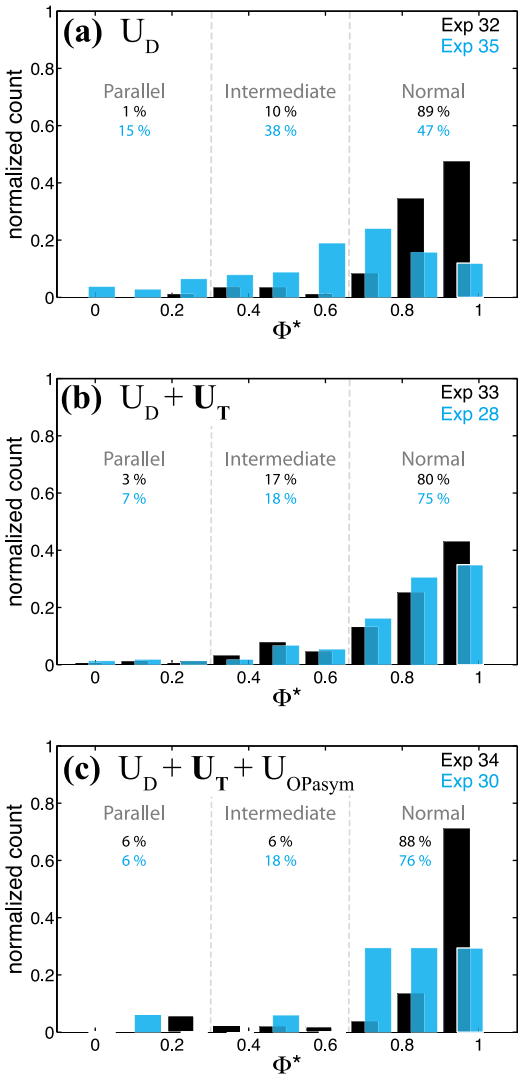

Figure 2. Histogram plots for normalized whisker count verses normalized whisker alignment (Φ*) at the end of an experiment (t* = 1). Bars in black are for experiments with initial (t* = 0) trench-normal whisker orientations ($\Phi_i^* = 1$) while bars in blue are for those with initial trench-parallel orientations ($\Phi_i^* = 0$). Corresponding percent alignments displayed in black/blue. (a) Downdip only cases (no rollback or extension) showing strong normal alignment only when whiskers are initially so oriented before the start of the experiment (Exp. 32). (b) Cases with translational rollback motion in addition to the downdip component. (c) Cases with translational rollback and asymmetric extension of the overriding plate in addition to the downdip component. Experiments with a rollback component show stronger trench-normal alignment regardless of initial whisker orientation.

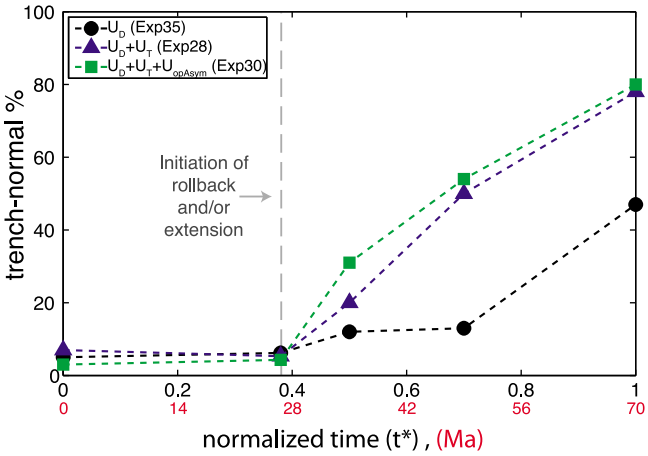

Figure 3. Trench-normal whisker percentage verses normalized time (t*) for the purely downdip (Exp35), rollback (Exp28), and rollback with asymmetric extension (Exp30) cases. Grey dashed line indicates the initiation of rollback and/or extension for the two later cases. Time is normalized by the length of each experiment with scaled mantle values displayed in red. All three cases begin with more than 90% trench-parallel alignment and evolve towards trench-normal with time. Strongest normal alignment occurs when there is a component of rollback motion, U_T (blue and green dashed lines).

vs. blue histograms) with the majority of whiskers (≥75%) aligned with the direction of subduction-induced flow.

4. Discussion

4.1. Strain Evolution

[11] Knowledge of the relationship between strain and anisotropy is essential for interpreting seismic observations in terms of mantle flow. Just as important, however, is the relationship between 3-D time evolving flows and strain [e.g., *Kaminski and Ribe*, 2002]. Assuming the olivine a-axis aligns in the direction of maximum shear flow (A-type fabric), our results suggest there are three geodynamic factors to consider when predicting mantle flow within subduction zones: (1) initial orientation of the fast axis, (2) style of subduction and (3) time evolution of the system. Interestingly, the initial orientation is most important for determining whether and how strain marker alignments can be related to the local pattern of mantle flow.

[12] We have shown in Figure 2 (black bars) that whiskers within the backarc wedge that are initially trench-normal remain oriented with the horizontal components of subduction-induced flow, regardless of subduction style. In such cases, factors such as style of subduction and time evolution are less important and anisotropy observations would be representative of the local mantle flow. For subduction systems where the initial orientation of the a-axis is not trench-normal, inferring mantle flow from anisotropy studies is less straightforward and does depend upon the aforementioned geodynamic factors.

[13] In the initially trench-parallel ($\Phi_i^* = 0$) downdip case (Figure 2, Exp. 35), alignment is quite variable even after 70 Ma of subduction, despite the relatively simple trench-normal flow field. Using passive micro-bubbles, horizontal velocity measured along trench (y-direction) in this scenario is essentially constant, with an average range of $0.25U_D$ (edge) to $0.3U_D$ (center) yielding weak horizontal shear (e.g., small velocity gradient, dU/dy). For simple downdip subduction, whisker alignment does not necessarily equate to direction of mantle flow and knowledge of the initial a-axis orientation is therefore important. In contrast, rollback cases had an average range of $0.4U_D$ (edge) to $1.0U_D$ (center), reflecting a larger shear flow towards the center that aligns strain markers in the direction of flow regardless of initial orientation. *Kincaid and Griffiths* [2004] reported similar rollback velocities in their investigation of circulation patterns and slab surface temperature (SST). They argued the horizontal shear flow in rollback cases focused advection towards the center of the system, increasing SST.

[14] In our models, this same rollback-induced shear more efficiently aligns markers of strain in the direction of flow as compared to the purely downdip case. However, alignments are very time-dependent making comparisons between seismic data and geodynamic flows complicated. Figure 3 shows trench-normal whisker percentage as a function of time for the initially trench-parallel cases ($\Phi_i^* = 0$) displayed in Figure 2 (blue bars). All three experiments begin with more than 90% parallel alignment (less than 8% normal) and evolve under the same subduction conditions until t* = 0.38. During this period of time, whiskers remain oriented roughly perpendicular to the direction of subduction-induced flow. After the initiation of rollback and/or extension (Exps. 28 & 30), horizontal shear increases the rate of alignment as compared to the purely downdip case (Exp. 35). By the end of an experiment ($t^* = 1$), more than 75% of whiskers in the rollback cases are trench-normal (e.g., aligned with the direction of flow) whereas in the downdip only case, the majority remain oblique to the direction of flow. Based on these $\Phi_i^* = 0$ end-member experiments, anisotropy observations during the first 30–50 Ma ($t^* \lessapprox 0.7$) would be a poor indication of the actual mantle flow, regardless of subduction style. Even in subduction systems with an initial random distribution (e.g., isotropic), alignment of whiskers is still predicted to appear variable during early stages of subduction-induced flow. Strain markers originally trench-normal (or very near) would quickly begin to reflect the local flow, however, those initially oriented in the intermediate to trench-parallel range would cause seismic observations to vary until later stages of subduction. Past and present plate motions should therefore be considered carefully when inferring mantle flow within the central regions of subduction.

4.2. Comparison With SKS Splitting Results

[15] The High Lava Plains (HLP) region of eastern and central Oregon of the Cascade subduction system in the Northwest U.S. offers a good opportunity to compare results of strain alignment from both the geodynamic models and seismic observations. We have demonstrated that both the initial olivine a-axis orientations (which link to past plate forcings) and the time varying subduction motions are important factors. The western U.S. margin has had a long history (~150 Ma) of subduction [e.g., *Severinghaus and Atwater*, 1990; *Bunge and Grand*, 2000], in addition to trench retreat which initiated around ~20 Ma after fragmentation of the Farallon plate and formation of slab windows

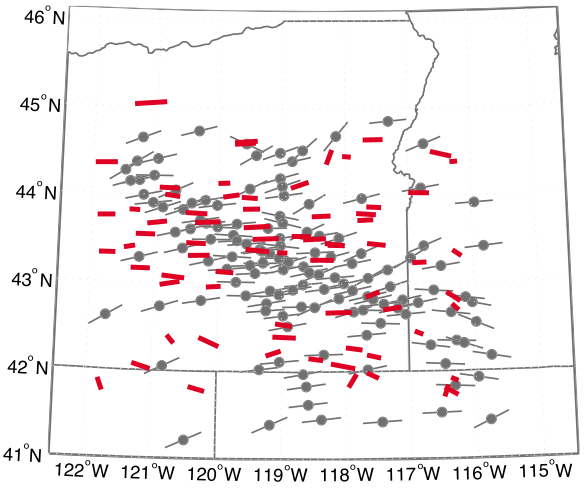

Figure 4. Comparison of the SKS splitting results (grey) with whisker alignment (red) under the HLP from the case with plate motions most like the Northwest U. S. (Exp. 34).

[*Atwater and Stock*, 1998]. As a result, initial orientation and time-dependency are less important and strain markers under the HLP are expected to have strong trench-normal alignment.

[16] SKS phases examined by *Long et al.* [2009] and this study exhibit large delay times (1.5–2.5 sec) and roughly E-W fast directions (Figure 4, grey lines). Stations to the north of 45N were not included in the comparison, as *Long et al.* [2009] demonstrated that there is a strong contribution from frozen lithospheric anisotropy at these stations. We compare these results to whisker orientations from the case with subduction motions most similar to the Cascadia system (Exp. 34), which includes trench rollback and asymmetric extension of the overriding plate (Figure 4, red lines). Due to the long history of subduction along this margin, we choose the model case where strain markers were initially oriented approximately trench-normal ($\Phi_i^* = 1$). However, as we have shown previously, initial orientation of whiskers in cases of mature rollback do not greatly alter late-stage alignments. It is important to note that in this initial study, laboratory measurements were taken over only one depth region (~90–150 km below lithosphere) whereas the seismic observations are a path-integrated value through the anisotropic upper mantle. Depth dependence of whiskers, as well as higher order complexities such as geometry and occurrence of oblique subduction in the Northwest U.S., will be important to consider in future modeling. Despite these factors, however, SKS splitting observations in the HLP are in good agreement with the experimental predictions.

5. Conclusions

[17] Our models have shown that relationships between mantle flow and anisotropy are complicated in subduction zones and important geodynamic factors such as (1) initial orientation of strain markers (e.g., olivine fast-axis), (2) style of subduction, and (3) time-evolving flow need to be considered. Connections between seismic data and flow in the central backarc wedge (away from slab edges) can be particularly complex during early stages of subduction or when the slab has little or no component of rollback motion. Rollback-induced horizontal shear causes predominantly trench-normal strain alignment in the backarc mantle wedge in contrast to longitudinal subduction which, despite the simple flow field, results in complex and variable orientations from the lack of strong horizontal shear. In the HLP, splitting observations are in good agreement with the trench-normal laboratory predictions of strain alignment. Comparison with future modeling of whisker alignment within buoyant plumes occurring near subduction-induced flow will help distinguish between proposed plume and non-plume tectonomagmatism in the Northwest U.S.

[18] **Acknowledgments.** We thank Ross Griffiths (Australian National University) for use of the Geophysical Fluid Dynamics Laboratory and Tony Beasley for expert technical assistance. Seismic data from the High Lava Plains and USArray Transportable Array networks were used in this study. We thank the network operators and the IRIS DMC for making the data available. The HLP experiment was led by Matt Fouch (Arizona State University) and David James (Carnegie Institution of Washington) and funded by the NSF-Continental Dynamics program. We thank the HLP project participants for useful scientific discussions as well as Martha Savage and two anonymous reviewers for their thoughtful and helpful reviews. MDL acknowledges support from NSF grant EAR-0911286 and KAD/CK acknowledge support from NSF grant EAR-0506857.

[19] The Editor thanks Martha Savage, James Conder and an anonymous reviewer.

References

Atwater, T., and J. Stock (1998), Pacific-North America plate tectonics of the Neogene southwestern United States: An update, *J. Geophys. Res.*, *40*, 375–402.

Bunge, H.-P., and S. P. Grand (2000), Mesozoic plate-motion history below the northeast Pacific Ocean from seismic images of the subducted Farallon slab, *Nature*, *405*, 337–340, doi:10.1038/35012586.

Buttles, J., and P. Olson (1998), A laboratory model of subduction zone anisotropy, *Earth Planet. Sci. Lett.*, *164*, 245–262.

Camp, V. E., and M. E. Ross (2004), Mantle dynamics and genesis of mafic magmatism in the intermontane Pacific Northwest, *J. Geophys. Res.*, *109*, B08204, doi:10.1029/2003JB002838.

Carlson, R. W., and W. K. Hart (1987), Crustal Genesis on the Oregon Plateau, *J. Geophys. Res.*, *92*(B7), 6191–6206, doi:10.1029/JB092iB07p06191.

Carlson, R. W., D. E. James, M. J. Fouch, T. L. Grove, W. K. Hart, A. L. Grunder, R. A. Duncan, G. R. Keller, S. H. Harder, and C. R. Kincaid (2005), On the cause of voluminous magmatism in the northwestern United States, *Geol. Soc. Am. Abstr. Program*, *37*(7), 125.

Christiansen, R. L., G. R. Foulger, and J. R. Evans (2002), Upper-mantle origin of the Yellowstone hotspot, *GSA Bull.*, *114*(10), 1245–1256.

Conder, J. A., and D. A. Wiens (2007), Rapid mantle flow beneath the Tonga volcanic arc, *Earth Planet. Sci. Lett.*, *264*, 299–307, doi:10.1016/j.epsl.2007.10.014.

Cross, T. A., and R. H. Pilger (1978), Constraints on absolute motion and plate interaction inferred from Cenozoic igneous activity in the western United States, *Am. J. Sci.*, *278*, 865–902.

Fischer, K. M., E. M. Parmentier, A. R. Stine, and E. R. Wolf (2000), Modeling anisotropy and plate-driven flow in the Tonga subduction zone back arc, *J. Geophys. Res.*, *105*(B7), 16,181–16,191.

Funiciello, F., C. Faccenna, D. Giardini, and K. Regenauer-Lieb (2003), Dynamics of retreating slabs: 2. Insights from three-dimensional laboratory experiments, *J. Geophys. Res.*, *108*(B4), 2207, doi:10.1029/2001JB000896.

Griffiths, R. W., R. I. Hackney, and R. D. van der Hilst (1995), A laboratory investigation of effects of trench migration on the descent of subducted slabs, *Earth Planet. Sci. Lett.*, *133*, 1–17.

Jordan, B. T., A. L. Grunder, R. A. Duncan, and A. L. Deino (2004), Geochronology of age-progressive volcanism of the Oregon High Lava Plains: Implications for the plume interpretation of Yellowstone, *J. Geophys. Res.*, *109*, B10202, doi:10.1029/2003JB002776.

Kaminski, É., and N. M. Ribe (2002), Timescales for the evolution of seismic anisotropy in mantle flow, *Geochem. Geophys. Geosyst.*, *3*(8), 1051, doi:10.1029/2001GC000222.

Karato, S., H. Jung, I. Katayama, and P. Skemer (2008), Geodynamic significance of seismic anisotropy of the upper mantle: New insights from laboratory studies, *Annu. Rev. Earth Planet Sci.*, *36*, 59–95, doi:10.1146/annurev.earth.36.031207.124120.

Kincaid, C., and R. W. Griffiths (2003), Laboratory models of the thermal evolution of the mantle during rollback subduction, *Nature*, *425*, 58–62.

Kincaid, C., and R. W. Griffiths (2004), Variability in flow and temperatures within mantle subduction zones, *Geochem. Geophys. Geosyst.*, *5*, Q06002, doi:10.1029/2003GC000666.

Kincaid, C., and P. Olson (1987), An experimental study of subduction and slab migration, *J. Geophys. Res.*, *92*(B13), 13,832–13,840.

Long, M. D., and T. W. Becker (2010), Mantle dynamics and seismic anisotropy, *Earth Planet. Sci. Lett.*, *297*, 341–354, doi:10.1016/j.epsl.2010.06.036.

Long, M. D., and P. G. Silver (2008), The subduction zone flow field from seismic anisotropy: A global view, *Science*, *319*(5861), 315–318.

Long, M. D., H. Gao, A. Klaus, L. S. Wagner, M. J. Fouch, D. E. James, and E. Humphreys (2009), Shear wave splitting and the pattern of mantle flow beneath eastern Oregon, *Earth Planet. Sci. Lett.*, *288*, 359–369.

Schellart, W. P. (2004), Kinematics of subduction and subduction-induced flow in the upper mantle, *J. Geophys. Res.*, *109*, B07401, doi:10.1029/2004JB002970.

Severinghaus, J., and T. Atwater (1990), Cenozoic geometry and thermal state of the subducting slabs beneath North America, in *Basin and Range Extensional Tectonics Near the Latitude of Las Vegas, Nevada*, edited by B. P. Wernicke, *Geol. Soc. Am. Mem.*, *176*, 1–22.

Wagner, L. S., D. W. Forsyth, M. J. Fouch, and D. E. James (2010), Detailed three-dimensional shear wave velocity structure of the northwestern United States, *Earth Planet. Sci. Lett.*, *299*, 273–284, doi:10.1016/j.epsl.2010.09.005.

Warren, L. M., J. A. Snoke, and D. E. James (2008), S-wave velocity struture beneath the High Lava Plains, Oregon, from Rayleigh-wave dispersion inversion, *Earth Planet. Sci. Lett.*, *274*, 121–131.

Xue, M., and R. M. Allen (2010), Mantle structure beneath the western United States and its implications for convection processes, *J. Geophys. Res.*, *115*, B07303, doi:10.1029/2008JB006079.

K. A. Druken and C. Kincaid, Graduate School of Oceanography, University of Rhode Island, South Ferry Road, Narragansett, RI 02882, USA. (kdruken@gso.uri.edu)

M. D. Long, Department of Geology and Geophysics, Yale University, PO Box 208109, New Haven, CT 06520, USA.